Search for a protocluster around a dusty starburst at z=4.2

Andrés Laza Ramos

Supervisor:
Helmut Dannerbauer

Index

List of Figures

List of tables

1 Introduction

1.1 Resumen

El estudio de protocúmulos de galaxias en un alto redshift (z>4) es necesario para poder comprender como las grandes estructuras del universo (cúmulos y super cúmulos de galaxias) se formaron en el universo temprano (alrededor de 1 G-años tras el Big Bang). Para poder encontrarlos, nos centraremos en la búsqueda de LAEs (Lyman-alpha emitters; galaxias emisoras de radiación Lyman-alfa, un tipo de radiación del hidrógeno dada cuando un electrón pasa del nivel n≥2 a n=1), ya que este tipo de radiación se observa en aquellas galaxias "jóvenes" con una gran formación de estrellas que están en proceso de formar cúmulos.

Este tipo de radiación se emite con una longitud de onda de λ=121.57 nm, pero debido al movimiento relativo entre estas lejanas galaxias y nosotros hay un corrimiento al rojo, debido al efecto Doppler, dependiente del redshift. Usando un objeto de referencia (HATLASJ142413.9+022304, también conocido como ID 141), con z=4.2 obtenemos, , que tal emisión la recibimos con una longitud de onda de λ=639.37 nm.

Para poder observarla, utilizaremos entonces los filtros creados para el programa SHARDS, en concreto U619/17, U636/17 y U653/17, de media banda, ya que son los óptimos para observar radiación en la longitud de onda deseada. Estos filtros se usan en el instrumento OSIRIS, instalado en el GTC (telescopio óptico-infrarrojo cercano de 10.4 m de diámetro). Tomaremos imágenes alrededor del objeto de referencia usando estos 3 filtros con el objetivo buscar LAEs candidatas a pertenecer a un protocúmulo alrededor del objeto de referencia, en un redshift de valor cercano al de este.

1.2 Precedents

Even before Principia was published (1687), the first astronomers, thanks to the use of telescopes, noticed that the "Heavenly bodies" were organized in groups or clusters. Once Newton's masterpiece was published, scientists were able to connect why these objects were close together, and started to see the bigger picture: stars, which formed the galaxies, were not the only one that were arranged in clusters, but those same galaxies later form groups and clusters between them. These structures containing hundreds of galaxies and diameters that can reach 10 Mpc are not even the

largest in the universe, being this title given in 1980 to superclusters, clusters of galaxy clusters, bonded all together by gravity.

The key point here is *time*, as these clusters, especially the ones at high redshift (z>4) that we study are good "history-tellers". Thanks to their observation we can extract information from the early universe, as the light we are receiving from them was emitted around a googol years ago. They are one of the first fingerprints of our universe, getting insight on how it came to be as we know it.

Nevertheless, before a group of galaxies become a galaxy cluster, they form what is known as a protocluster. As defined by Overzier in 2016, protoclusters are "non-virialized structures in the distant universe which will finally collapse into typical local galaxy clusters, virialized systems of a mass larger than 10^{14} $M_\odot$ (solar masses)."

Finding these structures will be our ultimate objective. Selecting and observing forming galaxy clusters can help us to understand the formation of the most massive structures in the universe, which are composed of thousands of galaxies. Those galaxies have an old, co-eval and metal-rich population, which suggest that they may have formed as starburst at high redshift (Pérez-González, 2014). Looking for this type of galaxies at high redshift (z>4 as stated before, or in time scale, objects that formed around 1 Gyr after the Big Bang) then is our best choice to find the desired protoclusters.

1.3 The Lyman series, Doppler effect and redshift. Observation wavelength

In the early universe, star-forming galaxies often are selected as Lyman-alpha radiation emitter (LAEs). Lyman emission is a hydrogen spectral series of transitions that occurs when an electron in a state equal or higher than n=2, goes to the ground state (n=1). The expression for the Lyman series, this is, the wavelength which the transition emits, can be derived from Bohr's hydrogen atom model. If we recall, the quantized energy levels according to this model are given by:

$$E_n = -\frac{13.6}{n^2}\ \text{eV}$$

where n refers to the electron's state. The difference of energy between two states must then be equal to the emitted photon energy:

$$\Delta E = E_n - E_k = h\nu = \frac{hc}{\lambda}$$

being h Planck's constant, ν the photon's frequency, c the light speed in the medium (e.g. vacuum) and λ the associated wavelength. It is well-known that the product between the two first is hc=1.2398·10^{-6} eV·m. Substituting and operating:

$$\frac{1}{\lambda} = \frac{-13.6}{1.2398\cdot 10^{-6}}\left(\frac{1}{n^2} - \frac{1}{k^2}\right) = 10.9695\cdot 10^6\left(\frac{1}{k^2} - \frac{1}{n^2}\right) = R_H\left(\frac{1}{k^2} - \frac{1}{n^2}\right)\ \text{m}^{-1}$$

This result is known as the Rydberg's equation while R_H is called the Rydberg's constant. In case of Lyman series, k=1. As usual with any emission series, the suffix *alpha* (α) is used for $n=k+1$, *beta* (β) for $n=k+2$, and so on. The Lyman alpha (Ly_α) emission, which we are most interested in, has an associated wavelength of 121.57 nm, whereas the Lyman limit (Ly_∞; the value of the wavelength when n goes to infinity) is 91.16 nm, therefore belonging all the Lyman radiation to the UV spectrum. Fig. 1 shows a typical LAE spectrum diagram.

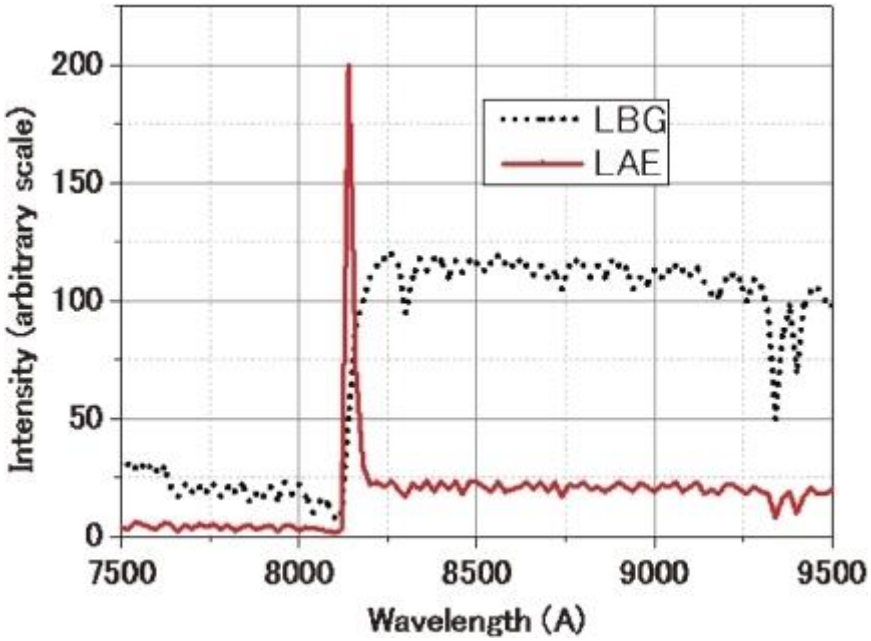

Figure. 1. Typical LAE emission spectra (thick red line). An LBG spectra line is also shown (black dotted line). Image taken from Iye M., 2011.

LAEs then emit at 121.57 nm, but due to the relative movement between us and them, we do not receive that emission at that same wavelength. This phenomenon is called the Doppler effect, and mathematically is defined as:

$$\Delta\nu = \frac{\Delta V}{c}\nu_0$$

where c and ν maintain their previous meaning (being ν_0 the emission frequency), while ΔV is the difference in velocity. Again, we are interested in wavelengths, so working out this expression using $c = \lambda\nu$ we obtain:

$$c\frac{\Delta\lambda}{\lambda_0^2} = \frac{\Delta V}{c}\frac{c}{\lambda_0} \quad ; \quad \frac{\Delta\lambda}{\lambda_0} = \frac{\Delta V}{c} = z$$

The coefficient of ΔV and c, z, is known as the shift. When it is larger than 0, this is, when the observed wavelength is larger than the emitted one due to objects moving away, it is called *redshift*, while when it is smaller due to objects moving to us, *blueshift*. Also, when this value gets closer (and overpass) ±1, it is said to be relativistic. A more popular form of the previous equation is:

$$\frac{\lambda_{obs}}{\lambda_{emi}} = 1 + z$$

that is easily calculated by writing λ_0 as λ_{emi} and $\Delta\lambda = \lambda_{obs} - \lambda_{emi}$, being the first the wavelength of the radiation emitted by the object and the second the wavelength of that same radiation seen by the observer

The question now is what our observed wavelength is. It is easily seen that it will depend on both the emitted wavelength and the redshift, being this second unknown[1] to us, needing then of a reference object. The celestial body fulfilling this task will be HATLASJ142413.9+022304, better known as ID 141 (Cox et al., 2011).

. ID 141 is a submillimetre galaxy (SMG; galaxies emitting with a wavelength between 1 mm and 200 μm; Smail, Ivison & Blain, 1997) belonging to the Herschel Astrophysical Terahertz Large Area Survey (H-ATLAS; Eales et al. 2010) cosmological survey, being one of the brightest sources detected in the Herschel deep surveys. Thought to be gravitationally lensed, its high redshift (z=4.243) has been well-determined thanks to the detection of carbon monoxide (CO) emission lines, which showed strong peaks (as seen in Fig. 2).

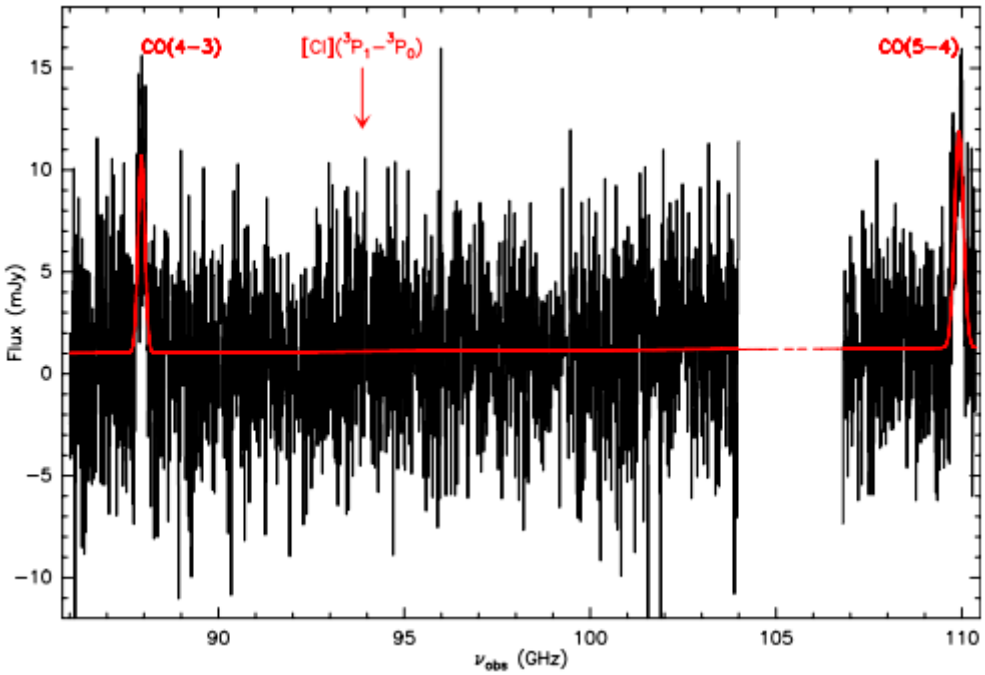

Figure. 2. Spectrum of ID 141, showing the CO detections (from 4 to 4 and from 5 to 4), done by Cox et al., 2011, with the Plateau de Bure Interferometer (PdBI).

Also, a property of ID 141 is that they have a high star formation rate (estimated to be (0.7–1.7) ×104 $\mu^{-1}LM_{\odot}yr^{-1}$.), making them excellent mass density peaks tracers and thus protoclusters tracers.

[1] In fact, the redshift is very known to us; we have talking about it since the project's title. However, it is in this context that is introduced.

Also, SMGs have been discovered to be associated to galaxy overdensities traced at other wavelengths, such as Lyα and Hα (Daddi, Dannerbauer et al., 2009; Walter et al., 2012).

Going back now to our previous expression, using ID 141's redshift and the emission wavelength of Lyα, we obtain that the observed wavelength is:

$$\lambda_{obs} = 637.39 \text{ nm}$$

which corresponds to a red colour in the visible spectrum. In order to observe this wavelength filters around this value must be used.

1.4 Telescope, instrument and survey

To aid us, we will use the filters conceived for the Survey for High-z Absorption Red and Dead Sources, most known as SHARDS, an ESO/GTC Large program (Pérez-González et al., 2013). SHARDS filters' wavelength range goes from 500 to 940 nm, while the band width goes from 14 to 34 nm. For our purpose, the filters used will be U619/17, U636/17 and U653/17, of respective wavelengths 619, 636 and 653 nm. They have a full width at half maximum (FWHM; the band width) of 15.8, 16.2 and 15.4 nm, respectively, what means that what the filter sees is half that value below and above their filtering wavelength. Our interest will be mainly in the images obtained with of the middle one as it is the closest to our reference wavelength, while the others will be used for checking.

SHARDS filters are used in the Optical System for Imaging and low-Intermediate-Resolution Integrated Spectroscopy (OSIRIS) the Day-One instrument installed in the Gran Telescopio Canarias. As its name implies, OSIRIS is used for observations in the visible spectrum, going its wavelength range from 365 to 1065 nm, and taking images from the sky using CCD cameras whose quantum efficiency (QE) reach 90% for 600 nm, making it the ideal instrument for our project.

Finally, Gran Telescopio Canarias (also known as GTC or GranTeCan) is not out of mention. The GTC is the largest optical-near-infrared telescope in the world, having a diameter of 10.4 m. Located at 2396 m above the sea level in the Roque de los Muchachos Observatory, in La Palma, this massive structure has been operating since 2009. Due to its huge collecting area (78.54 m^2) and fantastic location, it has been possible to observe some of the faintest objects in the night sky making great advances in astronomy, such as the deepest sky or the most recent one, the most distant star ever observed (up to this project date, 6-2018; GTC-IAC webpage, 2018).

Fig. 3. On the left panel, OSIRIS; on the right panel, the GTC with its dome opened at night. Images taken from the IAC webpage's archive.

2 Objectives

2.1 Resumen

Como ya dijimos, obtener galaxias candidatas a pertenecer a un protocúmulo será nuestro objetivo principal.

Para hacerlo, analizaremos las imágenes obtenidas con los filtros de SHARDS U619/17, U636/17 y U653/17 en una región del cielo alrededor de ID 141, de tamaño. Este análisis incluye la extracción y fotometría de las fuentes en las imágenes y una búsqueda de candidatos usando diagramas color-color, densidad de superficie e inspección visual. Para confirmar la validez de estos candidatos, espectroscopía de multi-objetos con OSIRIS será necesaria.

2.1 Objective of the project

As we stated before, the main objective of this work will be finding possible protocluster candidates which we will later examine.

We will do this by analysing images obtained using the U619/17, U636/17 and U653/17 SHARDS filters of a region of the sky. This analysis includes extraction and photometry of the sources in the images and a search of candidates using colour-colour diagrams, surface density calculation and visual inspection of these objects. To confirm the validity of these candidates, multi-object spectroscopy with the GTC-OSIRIS instrument is needed.

3 Methodology

3.1 Resumen

A continuación, describiremos la metodología utilizada para llegar hasta nuestro resultado final. Dividido en varias partes, empezamos primero analizando las imágenes (obtenidas por Dannerbauer y la reducción de datos de estas hecha por Pérez-González et al.) usando *Source Extractor* (SE), un software creado por E. Bertin con el objetivo de analizar imágenes FITS.

Para configurar este programa, debemos crear dos tipos de ficheros, uno con los parámetros de entrada (como valor del seeing, área mínima de detección, magnitud en el punto cero, etc.) que decidirán cómo funciona la detección. Otros refieren a las propiedades del catálogo o las imágenes de chequeo (nombre, formato) o directamente no influyen el tipo de análisis que realizaremos, por lo que no deberán cambiarse. El otro tipo de fichero nos da los parámetros de salida, que en nuestro caso serán el número del objeto, sus coordenadas (en la imagen y en el cielo), sus magnitudes (con sus errores), el tipo de objeto y ciertos parámetros para remarcarlos luego.

Para comprobar que la detección ha sido correcta, usaremos CHECK_IMAGE y archivos *.reg*, los cuales cargaremos en un software de visualización como DS9. Una detección correcta implica que no hay seleccionadas zonas de fondo sin ningún tipo de fuente.

Una vez comprobado los análisis, debemos clasificar los objetos, usando diferentes criterios: primero, debemos descartar todo objeto que SE no ha considerado galaxia; y segundo debemos "corregir" aquellos objetos no detectados o con un SNR demasiado bajo (menor que 3 según nuestro criterio).

Luego, para seleccionar nuestros posibles candidatos, crearemos diagramas color-color (basado en el modelo de Chanchaiwowarit et al., 2017) además de utilizar un catálogo (con objetos de GOODS-N) cedido por Arrabal et al. (2018), el cual contiene un gran número de LAEs en el rango de nuestro redshift, de modo que comparando un diagrama obtenido con este catálogo podemos seleccionar una zona en el nuestro que incluya mejores posibles candidatos.

Por último, una inspección visual se hace para comprobar que estos objetos están presentes en todas las imágenes y un análisis de multi-objeto se tendría que realizar para confirmar que son candidatos satisfactorios.

3.2 Analysis of the FITS images. Configuration files

Throughout this project we will mainly work with FITS images, so defining its concept shall be a priority. FITS, which stands for "Flexible Image Transport System", is a file format that allows us to store multiple types of data, as images, tables, etc. in a single file. This format is useful to modern day astronomers as it allows them to transport, among others, a 2D image of some sky region plus the header, a table which contains physical information about the telescope and the sky region. Our analysis will mainly consist on the study of the image and data extraction from the header.

The images that we are going to work with have been obtained by the IP Dannerbauer in service mode in ~9 hours of night time (2h 13m for U619/17, 1h 42m for U636/17 and 2h 55 min for U653/17, plus overheads) with a decreasing Moon, little clouds and a supposed seeing of 0.9 arcsec, whereas the data reduction was done by Pérez-González et al. using the SHARDS pipeline.

There are various tools to, given the FITS image, do its photometry. In our case, we will use Source Extractor (SE), a UNIX (or UNIX-like operating systems) software made by E. Bertin that allows us to obtain photometric and physical data from an image's objects, given some parameters of the FITS. The output information is given in the form of a catalogue, where each column represents a different extracted data and each file the value of that data for every detected object.

To make SE work one must create two specific files: a *.param* file, containing the information that we want to obtain; and a *.sex* file, which will contain the criteria SE will follow to do the data extraction. Each file has its own structure and a sample one, containing a rough explanation of the parameters, can be created via SE commands.

Beginning with the second one (see Fig. 4), the user must have the values here well-defined in order to have a proper detection and photometry of the images. For our project not all the parameters are needed. Those that we need to define are:

- **CATALOG_NAME:** name of the resulting catalogue, specified by the user.
- **CATALOG_TYPE:** data type of the resulting catalogue. There are assorted options (see Fig. 4), each one of different properties, while NONE is a "free format" (just the output data). The most useful to us are ASCII and ASCII_HEAD, both giving a catalogue in an ascii table (simple to manage) outputting the second one a header providing information of the image.
- **PARAMETERS_NAME:** name (including format, not necessarily *.param*) of the file containing the output data that the user wants to obtain.
- **DETECT_TYPE:** almost all images astronomers acquire nowadays are taken by a CCD camera. SE still offers the option of analysing the image of a photographic plate, which is not our case.
- **DETECT_MINAREA:** the minimum number of pixels an object must have to

```
# Default configuration file for SExtractor 2.19.5
# EB 2014-03-19
#

#------------------------------- Catalog ------------------------------------

CATALOG_NAME     test.cat       # name of the output catalog
CATALOG_TYPE     ASCII_HEAD     # NONE,ASCII,ASCII_HEAD, ASCII_SKYCAT,
                                # ASCII_VOTABLE, FITS_1.0 or FITS_LDAC
PARAMETERS_NAME  default.param  # name of the file containing catalog contents

#------------------------------- Extraction ----------------------------------

DETECT_TYPE      CCD            # CCD (linear) or PHOTO (with gamma correction)
DETECT_MINAREA   5              # min. # of pixels above threshold
DETECT_THRESH    1.5            # <sigmas> or <threshold>,<ZP> in mag.arcsec-2
ANALYSIS_THRESH  1.5            # <sigmas> or <threshold>,<ZP> in mag.arcsec-2

FILTER           Y              # apply filter for detection (Y or N)?
FILTER_NAME      default.conv   # name of the file containing the filter

DEBLEND_NTHRESH  32             # Number of deblending sub-thresholds
DEBLEND_MINCONT  0.005          # Minimum contrast parameter for deblending

CLEAN            Y              # Clean spurious detections? (Y or N)?
CLEAN_PARAM      1.0            # Cleaning efficiency

MASK_TYPE        CORRECT        # type of detection MASKing: can be one of
                                # NONE, BLANK or CORRECT

#------------------------------- Photometry ----------------------------------

PHOT_APERTURES   5              # MAG_APER aperture diameter(s) in pixels
PHOT_AUTOPARAMS  2.5, 3.5       # MAG_AUTO parameters: <Kron_fact>,<min_radius>
PHOT_PETROPARAMS 2.0, 3.5       # MAG_PETRO parameters: <Petrosian_fact>,
                                # <min_radius>

SATUR_LEVEL      50000.0        # level (in ADUs) at which arises saturation
SATUR_KEY        SATURATE       # keyword for saturation level (in ADUs)

MAG_ZEROPOINT    0.0            # magnitude zero-point
MAG_GAMMA        4.0            # gamma of emulsion (for photographic scans)
GAIN             0.0            # detector gain in e-/ADU
GAIN_KEY         GAIN           # keyword for detector gain in e-/ADU
PIXEL_SCALE      1.0            # size of pixel in arcsec (0=use FITS WCS info)

#------------------------- Star/Galaxy Separation ----------------------------

SEEING_FWHM      1.2            # stellar FWHM in arcsec
STARNNW_NAME     default.nnw    # Neural-Network_Weight table filename

#------------------------------- Background ----------------------------------

BACK_SIZE        64             # Background mesh: <size> or <width>,<height>
BACK_FILTERSIZE  3              # Background filter: <size> or <width>,<height>

BACKPHOTO_TYPE   GLOBAL         # can be GLOBAL or LOCAL

#------------------------------- Check Image ---------------------------------

CHECKIMAGE_TYPE  NONE           # can be NONE, BACKGROUND, BACKGROUND_RMS,
                                # MINIBACKGROUND, MINIBACK_RMS, -BACKGROUND,
                                # FILTERED, OBJECTS, -OBJECTS, SEGMENTATION,
                                # or APERTURES
CHECKIMAGE_NAME  check.fits     # Filename for the check-image

#--------------------- Memory (change with caution!) -------------------------

MEMORY_OBJSTACK  3000           # number of objects in stack
MEMORY_PIXSTACK  300000         # number of pixels in stack
MEMORY_BUFSIZE   1024           # number of lines in buffer

#----------------------------- Miscellaneous ---------------------------------

VERBOSE_TYPE     NORMAL         # can be QUIET, NORMAL or FULL
HEADER_SUFFIX    .head          # Filename extension for additional headers
WRITE_XML        N              # Write XML file (Y/N)?
XML_NAME         sex.xml        # Filename for XML output
```

Figure 4. The sample *.sex* file generated by SE.

be considered a detectible item. This is given by the limited telescope/instrument resolution and the seeing (specially in our case). Also, it must make physically sense, this is we need enough pixels to have an object contained and well defined.

- **DETECT_TRESH:** threshold of the detection. Objects will be detected only if their magnitude is above this value. Combined with the previous parameter they form the core of the detection.
- **PHOT_APERTURES:** one of the most important parameters, as it denotes the diameter (in pixels) that the output magnitude data (MAG_APER) we will obtain and use. To give a good value for this input, one must observe first the objects in their images and conclude which is the diameter containing most of the light in most of the object. As Table 2 shows (section [4.2]), in our case 7.5 px (1.91 arcsec) were chosen as the aperture radius for all the images.
- **MAG_ZEROPOINT:** the zero point of the instrument. The zero point is the magnitude at which an object produces one count per second in the detector. This value is different for each image, and contained in the header, which can be read using IRAF, SKYCAT (SKY), DeepSpace9 (DS) or other astronomy applications.
- **PIXEL_SCALE:** size of the CCD pixel, given in arcsec. This value is mostly found in the instrument's specifications. In case of OSIRIS, this value is 0.127", but as it has two chips, the standard observing modes use 0.254", value we have given to SE to perform the detections.
- **SEEING_FWHM:** the seeing in arcsec, specific to each image. The easiest way to obtain it is using the "Pick object" tool in SKY. As it will change depending on the object, an average value must be used.
- **STARNNM_NAME:** the file that will classify the objects in star-like and non-star-like. The file provided to execute this is in the SE directory, and it is good enough for almost any classification, including ours.
- **CHECKIMAGE_TYPE:** an output image SE offers to verify if detections were alright. We will deeply discuss this input parameter later, in section [3.3].
- **CHECKIMAGE_NAME:** name of the check image, if any (as it is in our case). Format (FITS, mainly) must be included. In section [3.3] will examine this parameter exhaustively.

Every other field can be left unchanged as it will not be necessary for our analysis. Table 2 (in the section [4.2]) contains the values we used for some of these parameters for each of the images.

Continuing with the *.param* file, this one is much more extended and customizable. Contrary to the *.sex* file, this one does not need to contain all the parameters but rather the ones we want an output of. The current version of SE (2.19.5) allow more than 400 extraction parameters, including over a dozen types of fluxes, and their associated magnitudes and errors. The ones we are most interested in (and will use) are:

- **NUMBER:** indexation of the detected objects, which will easy the classification.
- **FLUX_APER:** aperture flux; the flux contained in a circular contour of radius PHOTO_APERTURES and centre that of the object.
- **FLUXERR_APER:** the associated error to the previous magnitude.
- **MAG_APER:** aperture magnitude, the magnitude associated with the earlier flux.
- **MAGERR_APER:** the error related to this kind of magnitude.
- **X_IMAGE:** the x-coordinate of the object's centre in the image.
- **Y_IMAGE:** the y-coordinate of the object's centre in the image.
- **ALPHA_J2000:** the right ascension of the object, referred to the J2000s equinox.
- **DELTA_J2000:** the declination angle of the object, referred to the J2000s equinox.
- **CLASS_STAR:** the object type indicative, which we will deeply discuss in the following section ([3.4]).
- **BACKGROUND:** an average measure of the background of the detected object.
- **A_IMAGE:** semi-major axis of the ellipse-shaped object, given in terms of root mean squared noise (RMS noise).
- **B_IMAGE:** semi-minor axis of the ellipse-shaped object, given in terms of root RMS noise.
- **THETA_IMAGE:** angle of the ellipse-shaped object.

While the last three are only useful for the *.reg* file (*region* file; a DS9 specific[2] file that allows us to mark zones in a FITS image without modifying it) creation, which we will explain later (section [3.3]), and BACKGROUND to "fix" the image (the other output parameters will be used for classification.

One interesting property that the *.param* files have is that the wanted output parameters can be arranged in any order, as it structure is much simpler than the input parameters file: a document where each line is the wanted parameter, admitting also comments denoted by hashtags (#) as usual.

Once these files are conFig.d, the following command line must be written in the terminal to analyse an image with SE:

```
sex image -c conf_file.sex
```

This will trigger the identification and photometry process that will culminate in the creation of the catalogue. However, we are interested in a second type of analysis SE offers. SE allows to be given two images, do the detection on the first one while doing

[2] This type of file, or alike ones, can actually be used in other programs such as FUNTOOL or CIAO, or be exported from those to DS9 (with slight modifications).

the photometry on the second. The reason why we want this is that we are mostly interested in objects detected in the U636/17 filter as previously stated it is the filter on which the Lyα emission should fall (for the given redshift). It is essential for this process to have the images well aligned, if one does not want to have an erroneous output, which is also given in the shape of a catalogue. One must note that as photometry is done in the second image, the configuration file must be its. To run this mode in SE:

```
sex image1,image2 -c conf_file2.sex
```

This process must be done twice, both times with the U619/17 filter FITS as the first image and U619/17 and U653/17 filter FITS as second images, obtaining a catalogue for each time and a third from the U636/17 filter image. As the reference image was the same for all catalogues, they all contain the same number of objects Combining the three resultant catalogues we obtain a final catalogue containing all the objects detected in the U636/17 filter as seen with this filter and the U619/17 and U653/17 filter.

3.3 Detection checking. Check image and *.reg* files

Once finished the detection, a "sanity check" should be done to see if SE did it correctly. The best way to confirm is via the CHECK_IMAGE and *.reg* files.

Starting with the first one, the CHECK_IMAGE is an option in the *.sex* file that allows us to obtain up to 16 images (choosing between several file formats) of the detection process. These images can be of several types outlining different regions of the original image. There are 12 total modes for the CHECK_IMAGE (including not obtaining one), being our interest put in the mode APERTURES, and an image with subtracted background and the MAG_APER and MAG_AUTO integration limits (this is, with the objects delimited by a line), respectively. Drawbacks of the check images, especially the APERTURES ones, are that the ellipse they draw have the PHOT_APERTURES radius, which combined with the fact that it is marked with high-valued pixels in the image, it will not be seen in objects bigger than that radius. Fig. 5 shows some CHECK_IMAGE modes.

On the other hand, *.reg* (standing for *region*) files are not obtained but created. These files are quasi-equivalent to an APERTURES CHECK_IMAGE, without the background subtraction and more customizable. The *.reg* file must be programmed by the user following DS9's region description rules, which allows us to draw ellipses, boxes, text, vectors and other, changing their properties (size, colour, etc.). We will use ellipses, principally. *.reg* files solve the problem that the CHEK_IMAGE had, while one disadvantage is that to draw the ellipses around the objects one must give not only the position of the centre but also the semi-radii length and inclination angle. Thankfully for us, as stated before we can obtain these parameters for each object using SE, easing our job.

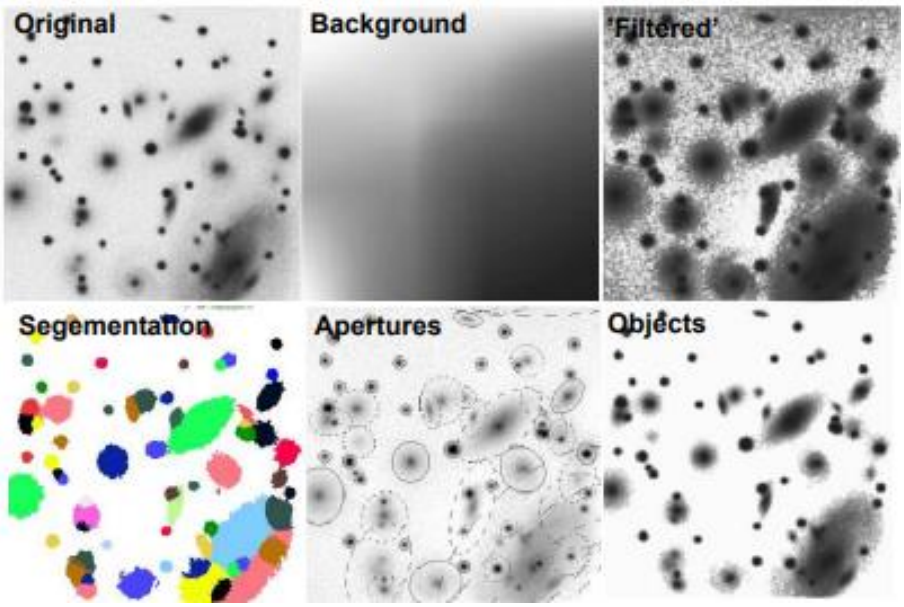

Figure 5. Different CHECK_IMAGE types. Image taken from the unoffcial SE guide.

3.4 Objects classification

We are only interested in galaxies, therefore those object that are stars must be discarded. To select those that are of our interest, some criteria must be chosen. This process is done in two steps: first we organize the objects by type and detection; and secondly, we impose some conditions to those that pass the first test to see if they are protocluster candidates.

In order to know what kind of object we are observing, one must be already thinking about the CLASS_STAR parameter value, critical to determine if the detected item is likely a star or a galaxy. The SE user's manual establishes that the output value will be between 0 (non-star object) and 1 (star) but does not specify what kind of object we have with a value halfway this range. To obtain the cut-off value that separates probable-star objects from those that are probably not, we must use some visualization software that give us the coordinates of the pixels, as we need to compare the shape of the objects with the value given by the CLASS_STAR value. This "visual inspection" will be done manually. Good candidates for this task are DS9 or SKY. The best way to proceed is to the image's catalogue and compare the CLASS_STAR value with the shape of the object that it belongs to, until one can certainly distinguish between stars and non-stars. The cut-of value we obtained was 0.906.

Another value to consider is the error in the magnitude (MAGERR_APER) as this value is directly related to the signal-to-noise ratio (SNR, S/N). When doing a detection, we define the signal (S) as the number of photons that are detected by the CCD (not all the photons that arrive are detected as our QE is not 100%), while the noise (N) is the total random contributions added to the detections from diverse

sources (i.e. electric origin). Basically, signal is the flux measured by the detector and noise its error, therefore the SNR determines the quality of the detection so that a higher value means a better measurement. As magnitude is defined as:

$$m = -\frac{5}{2}\log_{10}(S)$$

and its root mean square (rms):

$$\sigma_m^2 = \left(\frac{\partial m}{\partial S}\sigma_S\right)^2 = \left(\frac{-5/2}{\ln(10)}\frac{N}{S}\right)^2 = \left(\frac{-1.086}{S/N}\right)^2 \quad ; \quad \sigma_m = \frac{1.086}{S/N}$$

being this result the error associated to the magnitude, which is approximately the relative error in the measurement. In our case, we selected a SNR with a value of 3, which means that every detected object with a bigger error than 0.363 mag cannot be considered as a detection.

All the objects detected in U636/17 have a SNR larger than 3. However, this is not the case for U619/17 and U653/17, so an "upperlimit" must be defined. Upperlimit objects are all those objects in the catalogue which error correspond to a SNR=3, therefore their magnitude must be approximately the same. Table 3 (in section [4.2]) contains the value of the upperlimit magnitudes in the U619/17 and U653/17 filters images. As stated in the previous paragraph, all objects with a SNR lower than this are considered non-detected objects.

Finally, one must consider "pure" non-detections. Non-detected objects are those items that when the crossed photometry is done, SE detects them in the reference image however is unable to do its photometry in the second image (as it is not visible in it). They are easily identifiable as they will be denoted with "absurd values" in flux and magnitude (i.e. a magnitude of 99) in the catalogues.

The non-detections are not discarded from our catalogue despite their erroneous values, instead they are "fixed". By fix we mean that their magnitude value is changed to the one of their respective upperlimit. Generally, these objects are said to have no error after the fix, however for our calculations we will consider they have an error equal to the upperlimit error (this is, 0.363 mag).

3.5 Selection criteria

Once we have confirmed that our detections are correct, we must adopt some model that allows to distinguish which objects are in the desired redshift range, between z=4.16 and z=4.30. Initially, we had thought of using the one given by Bunker et al. (1995), consisting on a colour difference equation and an equivalent width calculation, however this model was conceived for magnitudes measured in broadband filters and narrowband filters, this is, filters whose FWHM differ widely, contrary to our case.

Therefore, another criteria must be followed. Based on the model presented by Chanchaiwowarit et al. (2017), we will use a reference catalogue to search for our protocluster candidates. We will represent colour-colour diagram with both, data taken from our catalogue and data taken from another catalogue containing galaxies in our redshift range and LAEs (also in the redshift range)

Our colour indexes will always consist on the subtraction of the magnitude obtained using the U636/17 filter to the one obtained with the other filters. When plotting the colour-magnitude diagram, the magnitude in the horizontal axis will be the one belonging to the U636/17, as it is the filter where the Lyα will mainly fall. This is personal choice that do not affect the results (if all plots are done using the same rule).

The catalogue used for the comparison, lent by Arrabal et al., 2018, contains information from over 1500 objects from the Great Observatories Origins Deep Survey North (GOODS-N) field observed using the same filters that we have used. As stated before, this data includes the redshift of the galaxies, and the presence of Lyman emission (whether if it a LAE or a Lyman-break galaxy; this is, a galaxy which Lyman emission disappear when viewed through certain filter). By doing and identical analysis with the data contained in this catalogue we will be able to obtain some diagrams to compare with ours.

This catalogue, conceived for surveying simultaneously LAEs and Lyman-break galaxies (LBGs) for the first time using all the medium band filters of SHARDS, contains a total of 1558 galaxies, being 528 of them LAEs. However, not all the galaxies included are useful to us, as some of them were not detected in some of our trio of filters. Contrary to our catalogue, we cannot treat these undetected objects as upperlimits and therefore must be discarded if not detected in one of the filters. For our analysis, only objects located in the 3 filters images were used. Table 1 contains information of our interest about the objects in this catalogue.

Valid objects (all): 1006		**Valid objects (redshift range):** 115	
LAEs	**LBGs**	**LAEs**	**LBGs**
295	102	21	102

Table 1. Detected objects in Arrabal et al.'s catalogue. Note that some LAEs are also LBGs (and therefore are included in the LBGs count. Fig. 13 in the annex shows a colour-colour diagram (in the annex, section [7.2]) of these objects only.

The surface density of LAEs in this catalogue, noting that the effective of the region observed was 128.4 arcmin^2, is 2.30 LAEs/arcmin^2 for all valid objects while 0.16 LAEs/arcmin^2 for those valid objects in redshift range. It is this second value we will use as a comparator.

3. 6 Comparison and protocluster candidates observation

Once we have achieved plotting all the data from both catalogues in all the desired manners, we can start looking for our candidates.

When the LAEs, LBGs and redshift range galaxies are plotted in the diagrams using the lent data, a region where the majority of LAEs in redshift range should appear. The protocluster candidates must be looked for in the same region in our plots.

Once we have delimited that zone, all the objects inside its should be selected and plotted using a *.reg* file in the U636/17 filter FITS. Again, a visual inspection should be made to search for those galaxies that appear to be nearby one another. Also, this same *.reg* file should be loaded into the other two filters FITS, to check if these candidates appear in them.

It must be noted that this visual inspection is a first step to find some possible candidates, fulfilling one of the aims of our project, however it is not enough to confirm that those galaxies do indeed belong to a protocluster. A further analysis on them should be done, as previously mentioned. We talk about this subject in section [5.2].

4 Results

4.1 Resumen

Presentamos ahora los resultados obtenidos tras la aplicación de los métodos descritos en la sección anterior.

Observando tanto las CHECK_IMAGE como los archivos *.reg*, se comprueba que la extracción de fuentes ha sido muy completa, observándose que en los bordes de la imagen hay incluso demasiados objetos. Estos aparecen debido a una corrección hecha sobre la imagen, de manera que son descartados (evitando coger cualquier objeto a menos de 100 píxeles del borde de la imagen).

Con todo esto, de los 6300 objetos inicialmente detectados, solo 3501 están más allá del perímetro válido y son, además, galaxias. Estos objetos tienen que analizarse más a fondo, comparándolo sus diagramas color-color con aquellos obtenidos con los datos de Arrabal et al..

En estos diagramas, se observa que la mayoría de LAEs en rango de nuestro redshift (el cual recordamos que va de z=4.16 a z=4.30 debido al FWHM del filtro U636/17), caen en una zona cuya diferencia de color entre U619/17 y U636/17 va de 1 a 4.3 mag y de 0.25 a 1.4 mag entre U653/17 y U636/17.

Cuando miramos esta región en nuestros diagramas, vemos que la cantidad de objetos es mucho menor, además de que carecemos de objetos en nuestro diagrama a partir de 2 mag en el eje vertical. Esto nos lleva a pensar, teniendo en cuenta la cantidad de objetos no detectados y upperlimits que se observan en ambos diagramas, que haya una posible contaminación de estos en los catálogos, los cuales podrían ser candidatos. Debe notarse, además, que entre aquellos objetos bien detectados en las 3 imágenes, todos tienen un SNR bastante bajo.

Haciendo una inspección visual de los objetos en esa región de nuestro catálogo, observamos que 2 de los objetos bien detectados y 10 de aquellos con algún upperlimit/non-detection pueden ser candidatos.

Por último, estudiando la densidad de superficie, de valor 0.08 LAEs/arcmin^2 es menor que la de Arrabal, de valor 0.16 LAEs/arcmin^2, muy baja para poder asegurar la existencia de protocúmulo.

4.2 Data obtention and extraction verification

Table 2 shows the objects detected in each image, alongside with some input parameters used in the detection. All these parameters have been obtained as explained in section [3.2]. Fig. 6 shows the region of the sky in which we are searching for the protoclusters candidates.

Image (corrected)	Detected objects	Aperture diameter (px)	Seeing (arcsec)	Zero-Point (mag)
U619/17	7457	7.5	0.96	32.83
U636/17	6300	7.5	1.07	33.01
U653/17	7570	7.5	0.99	33.33

Table 2. Detected object in each image, with some parameters used in the detection.

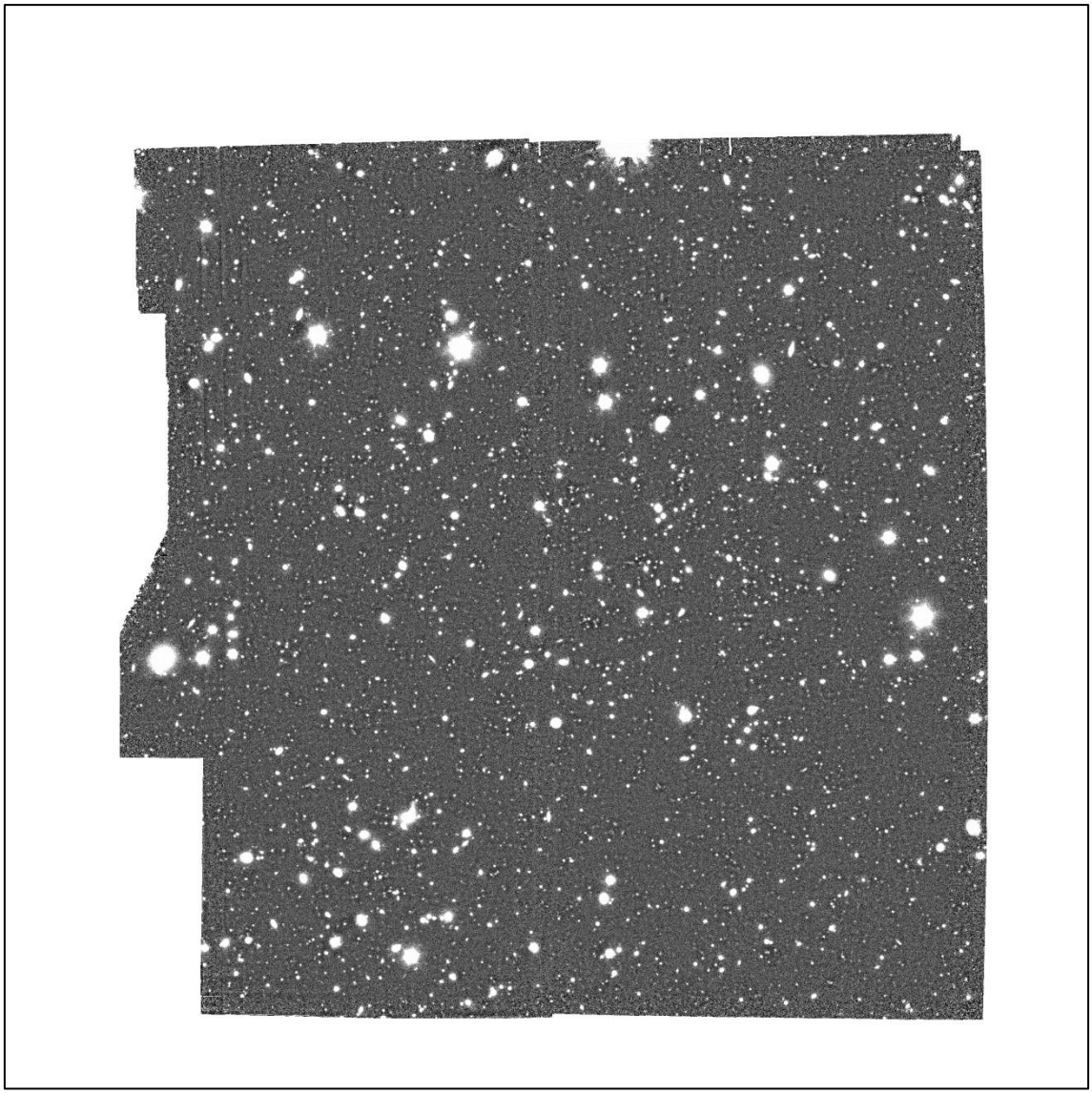

Figure. 6. FITS image obtained with the U636/17 filter. Note that the border of the image, of irregular shape, has a value of infinite (counts). The total size of the image (not counting the infinite value border is ~8.95'x8.8'.

To check if this extraction was correct (this is, to confirm that we used the correct input parameters and all objects were detected) we used the previously described check image. Fig. 7 shows the resulting check image obtained for our filter of most interest, U636/17. We can confirm that the extraction was successful as all the objects were detected and no wrong detections (i.e., a zone only having background noise was marked) were made. However, it must be mentioned that near the border of the image, too many objects were detected, possibly due to our correction of the infinite value border. To avoid contamination from these objects, all object separated 100 px or less from the edge was discarded.

Having the analysis succeed in all the images, the cross-image extraction (this is, the double image SE explained in section [3.2]) could be made and the final catalogue we would analyse was obtained.

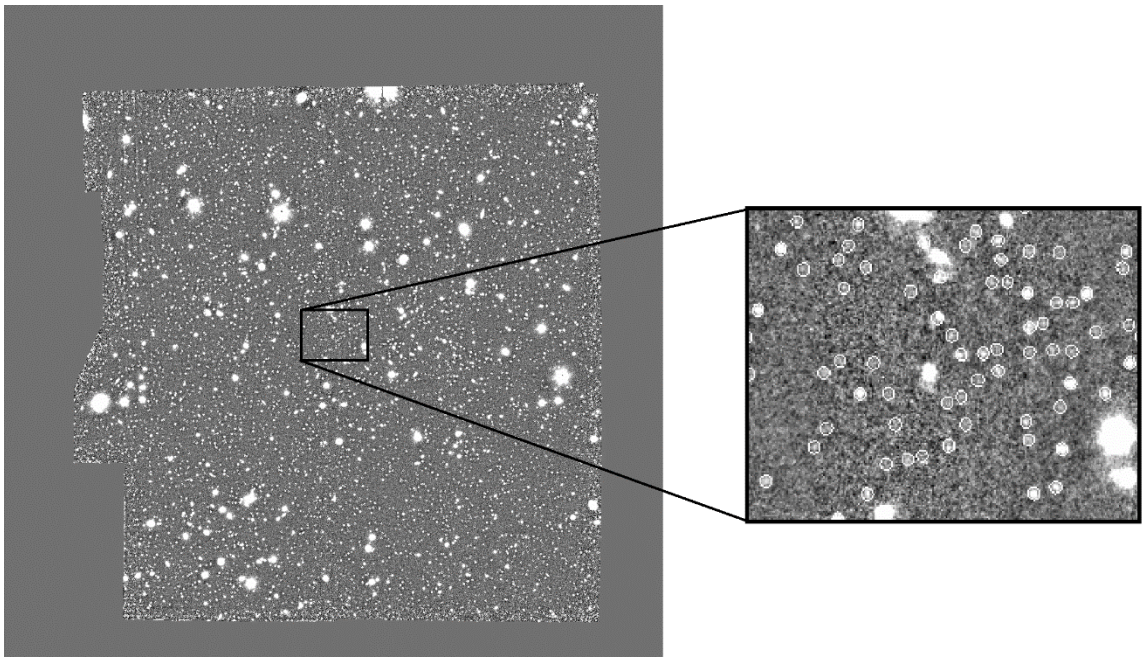

Figure. 7. Check image of the U636/17 filter before the correction. In the zoom in section the detected objects are sourrounded by the a circunference of the aperture radius. Larger objects also have this delimitation however it is not visible as it is not big enough to sorround them. It must be noted that the original image had it border (of white colour in Fig. 5) "fixed" average background value in order to obtaine the check image. The image have the same surface as the one in Fig. 6, while the surface of the zoomed region is ~0.67'x1.19'.

4.3 Data analysis

We must now classify the objects obtained according to the criteria mentioned in section [3.4]. First, we must consider the CLASS_STAR parameter value. We obtained, by a visual checking on objects in the U636/17 filter FITS that all objects with a value equal or lower than 0.906 in this field was most likely a galaxy. Together with the border cutting, the number of valid objects was reduced from 6300 to 3501.

Then, the upperlimit magnitude was identified for both the FITS of U619/17 and U653/17. We used a SNR=3 thus objects in the upperlimit will have a magnitude error of 0.363 (according to the expression in section [3.4]). All objects with an error larger than this value was considered a non-detection.

Also, we must consider those pure non-detected objects (if we recall, those objects present in the reference image and not found in the analysed ones), marked with a magnitude value and error of 99.

All non-detections (by SNR or pure) will have their magnitude fixed to the one of the upperlimit. Table 3 shows information about the upperlimit and non-detected objects in the U619/17 and U653/17 filters images.

Image	Upperlimit magnitude (mag)	Objects with SNR<3	Pure non-detected objects	Total non-detected objects
U619/17	26.76	123	45	168
U653/17	26.60	164	46	215

Table 3. Non-detected objects in the U619/17 and U653/17 filter images. It must be noted that the total objects detected (before dismissing those above the CLASS_STAR value and near the border) now was 6300 as the U636/17 filter image was used as the reference image.

Before plotting our data in the colour-colour diagram, an analysis of the data lent by Arrabal et al. was made, to know where to look for our protocluster candidates in our plots. We are mostly interested in those objects in redshift range that are LAEs (and secondly, LBGs), so we must look for any overdensity of these galaxies in the diagrams. Plotting the detected galaxies, the diagrams in Fig.s 8 and 10 (top panel) were obtained.

When looking at the colour-colour diagram it presents a clear region where LAEs are gathered (see Fig.s 8 and 10 [top pannel]). We therefore selected the region going from 0.25 to 1.4 mag in the x-axis and from 1 to 4.3 mag in the y-axis (see Fig. 10). The reason behind choosing this zone taking out some LAEs is to avoid the highly-dense region consisting of galaxies that are not in the redshift range, as it would do nothing but contaminate our sample.

Having this sample in mind, we plotted our colour-colour diagrams, shown in Fig.s 9 and 10 (bottom panel). Table 4 contains information about the objects in our catalogue contained in the selection region.

Total	Upperlimit only in U619/17	Upperlimit only in U653/17	Upperlimit in U619/17 and U653/17	Well-Detected
69	7	14	34	14

Table 4. Objects contained the selection region of the colour-colour diagram. Well-detected refers to those galaxies that lack an upperlimit in both, U619/17 and U653/17

Studying the colour-colour diagrams (Fig.s 8, 9 and 10; all of them scaled), especially the selection region, we observe how mostly of our well-detected galaxies fall below the zone where most of the LAEs are in the reference catalogue. This is possibly cause by a displacement of the magnitudes (also observed in the colour-magnitude diagrams, in the annex, section [7.2]), the previously mentioned contamination or both, which complicates obtaining satisfactory results.

More colour-colour and colour-magnitude diagram can be seen in the annex, section [7.2]. These diagrams were not used in order to obtain the final conclusions however they are truly useful in order to observe different galaxy classifications.

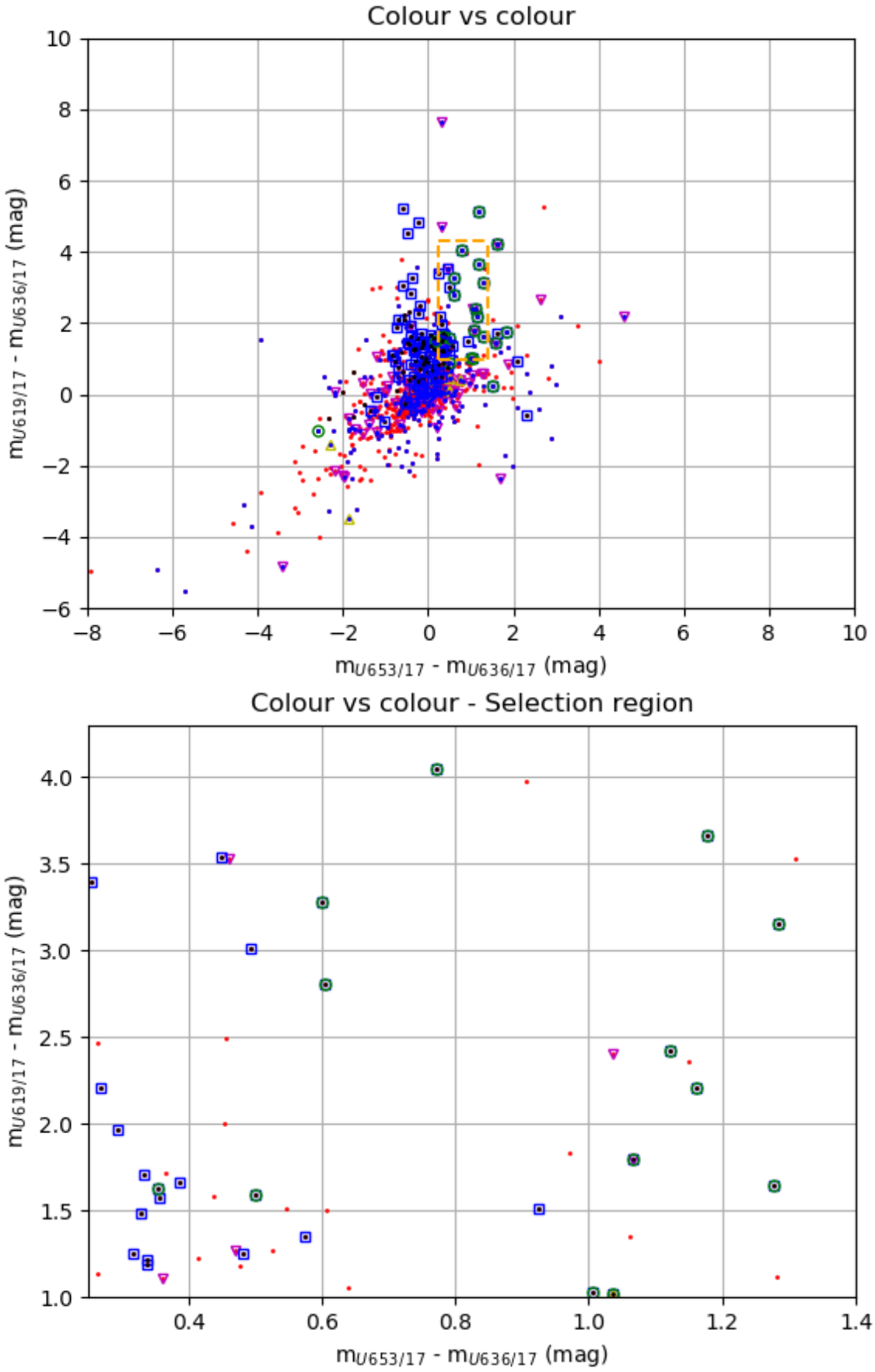

Figure. 8. Colour-colour diagram for Arrabal et al.'s catalogue. Red dots are used for all objects; black dots for those in z-range. Triangles refer to the upperlimits (yellow: U619/17; magenta: U653/17). Blue squares denote LGBs and green circles LAEs, in redshift range. In the top panel, all the detected galaxies in that catalogue, being the selection region dahsed in orange. In the bottom panel, the same diagram zoomed, showing the selection region.

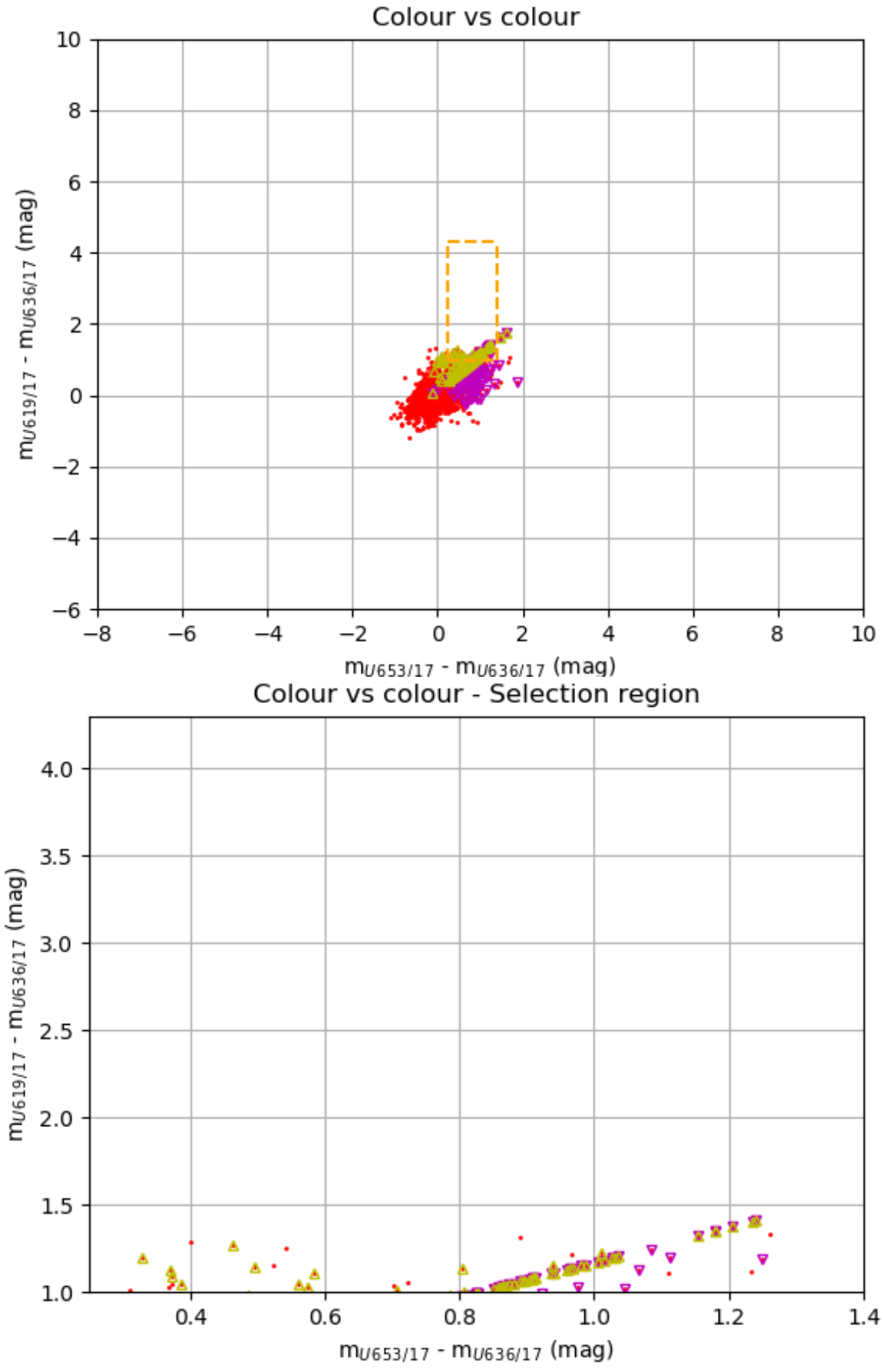

Figure. 9. Colour-colour diagram for our catalogue. Same legend as in Figure. 8.. In the top panel, all the detected objects. In the bottom panel, the same diagram zoomed, showing the selection region.

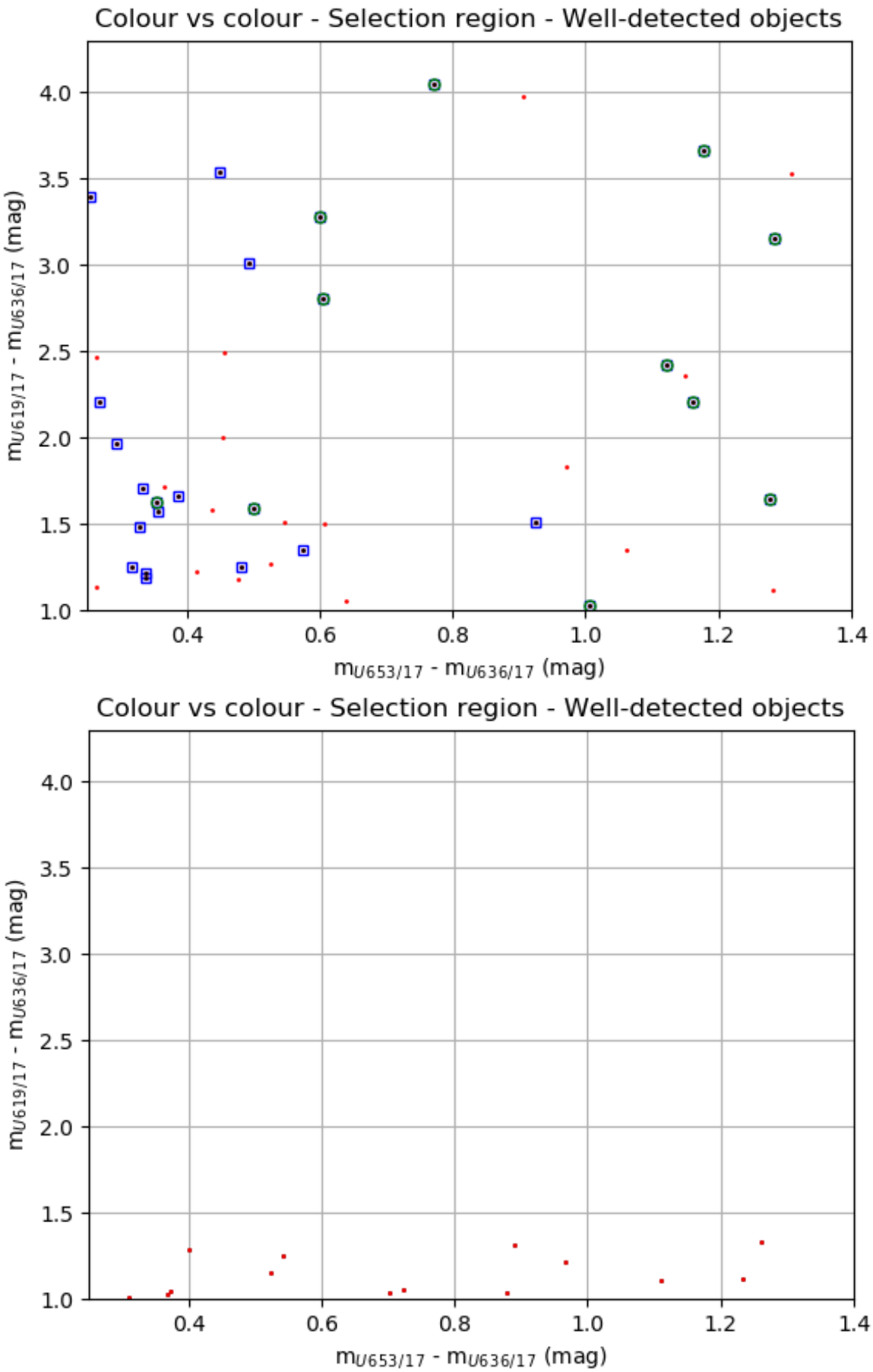

Figure. 10. Selection zone in both diagrams, showing well-detected objects only. Top pannel shows the Arrabal et al.'s region while bottom panel shows ours. Note the difference in quantity and distribution of galaxies.

Finally, taking all this into account, a further analysis on these objects was made, in order to know how reliable they were. To do so, we classified the galaxies by their magnitude error in the U636/17 filter. Fig. 11 shows the result of these classification.

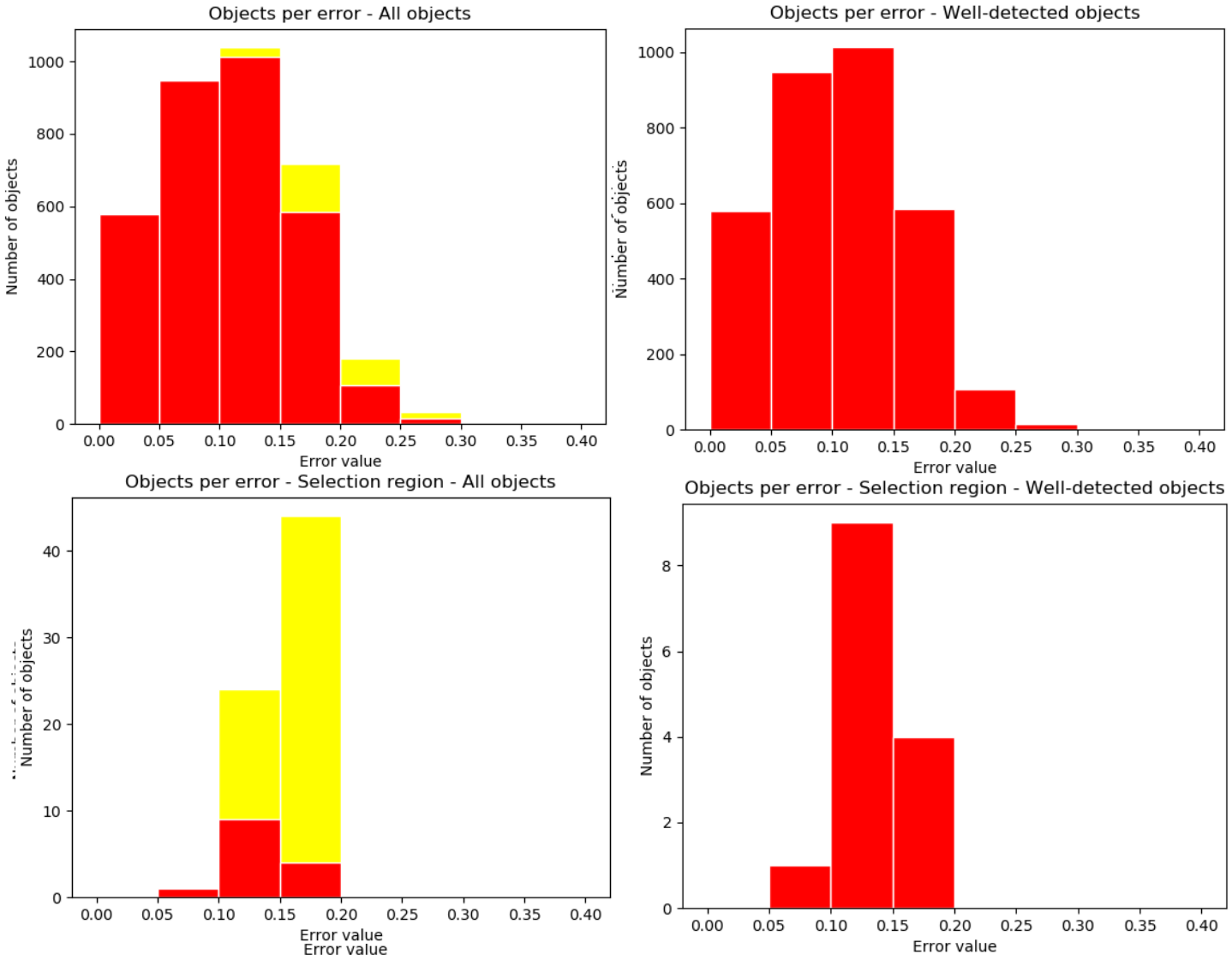

Figure 11. Histograms showing the number of objects per magnitude error (in filter U636/17). Top left panel shows all the detected objects, being yellow for those in any upperlimit. Same legend was used for the rest of the panels. Top right shows all the well-detected objects. Bottom left show all the objects in selection region, and bottom right only those well detected in that same region.

It is observed how, in general, most objects have an error between 0.10 and 0.15 mag (which means a SNR between 10.89 and 7.26) in U636/17. Considering all the possible contamination, and the faintness of the galaxies in general, these values are good yet improvable.

4.4 Visual checking

The best way to check if these galaxies are protoclusters candidates is to inspect them in the 3 filters images. To do so, we created a *.reg* file containing the well-detected galaxies and another *.reg* file containing the upperlimits/non-detections in that same region. We did this due to the large number of the lasts appearing in the selection region (greater than well-detected objects which made us suspect of a possible contamination as previously stated). The visual inspection must be done in the 3 images.

We must discard as possible candidates those objects that are not clearly seen in the 3 images and keep those that are, whether they are considered well-detected or not. Table 5 shows more information about the objects that passed this visual inspection. Image 12 shows these galaxies.

Object	$m_{U619/17}$	$\sigma_{mU619/17}$	$m_{U6363/17}$	$\sigma_{mU636/17}$	$m_{U6539/17}$	$\sigma_{mU653/17}$
1713*	26.27	0.23	24.94	0.09	26.02	0.25
2555	>26.76	---	25.56	0.15	>26.59	---
2766	>26.76	---	25.62	0.16	>26.59	---
3005	>26.76	---	25.49	0.14	25.96	0.20
3599*	>26.76	---	25.39	0.13	>26.59	---
3642	>26.76	---	25.63	0.16	26.43	0.31
4649	26.53	0.29	25.34	0.12	>26.59	---
4660	>26.76	---	25.53	0.15	26.54	0.35
5095*	26.52	0.29	25.27	0.12	25.81	0.18
5653	>26.76	---	25.41	0.13	>26.59	---
5739*	>26.76	---	25.36	0.13	>26.59	---
5914*	>26.76	---	25.35	0.12	>26.59	----

Table 5. Possible protoclusters candidates. $m_{U6XX/17}$ refer to the magnitude in that filter, while the next column to its error (in that same filter). "---", then the object was a non-detection in that filter. 2 of these galaxies (1713 and 5095) are well detected, while the other 10 have at least one upperlimit. Finally, objects having an asterisk (*) are the ones that were best visualized during the inspection.

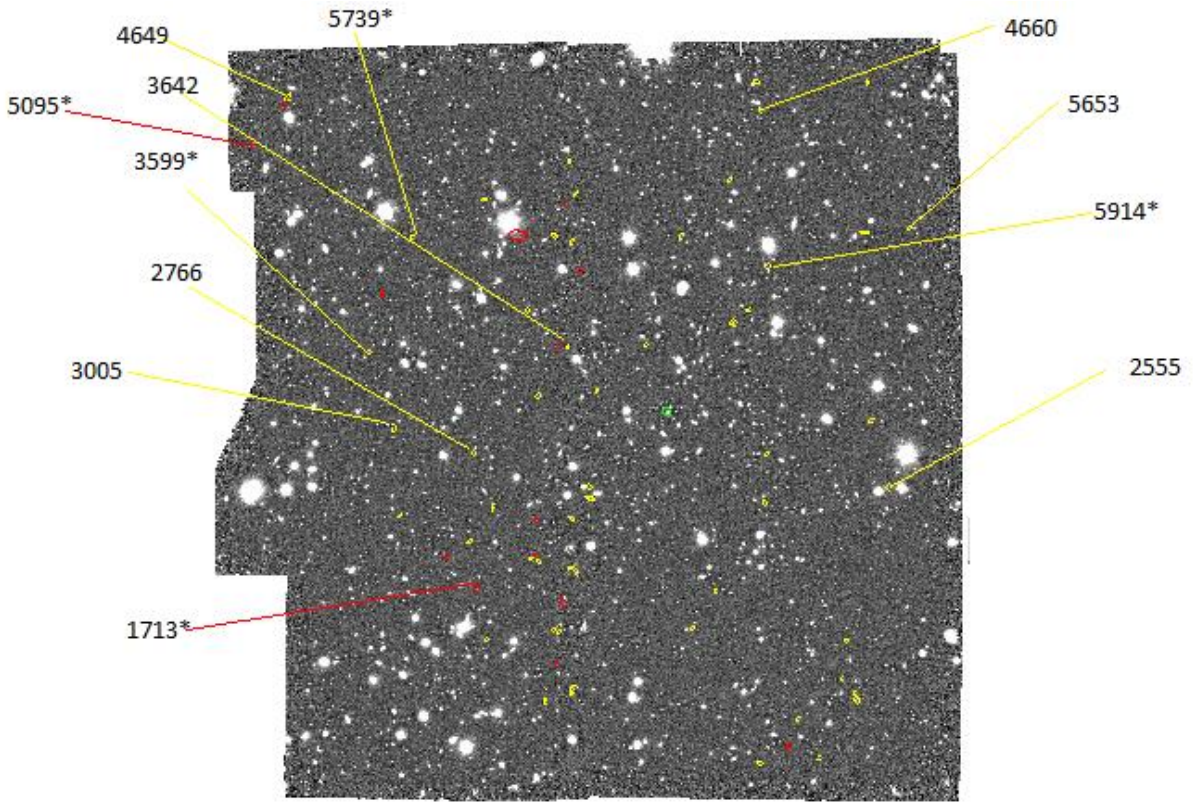

Figure. 12. *.reg* file in the U636/17 image, showing all objects in the selection region and marking those possible candidates. In red, the well detected objecs; in yellow, those objects with ate least one upperlimit/non-detection in one image; in green, ID 141.

Then, we must talk about the surface density. Our effective surface, taking into account the discarded border, measures 64.11 arcmin^2. In order to calculate the surface density, we have taken only those objects marked with and asterisk in Table 5, as are the most probable to be our candidates. Thus, a surface density of 0.08 (possible) LAEs/arcmin^2. This surface density is too small to for these galaxies to be considered part of a protocluster. Considering all the objects in Table 5 we obtained a surface density of greater value (0.19 LAEs/arcmin^2) however less reliable as the used objects have a worse resolution in the 3 images.

Finally, a surface density of LAEs in Arrabal et al.'s catalogue using galaxies with a $m_{U636/17}<26.78$ mag was done to compare too. This value of the magnitude was chosen as it the highest value for the magnitude in the U636/17 filter in our catalogue, whereas it can be seen in Fig. 14 and 15 in the annex (section [7.2]) that Arrabal et al.'s colour-magnitude diagrams go beyond that value however ours do not. The value obtained was 0.10 LAEs/ arcmin^2, slightly similar to the one we obtained. This fact supports our contamination idea.

5 Conclusions

5.1 Resumen

Hemos hecho un análisis de una región del cielo, buscando un posible protocúmulo de galaxias. Primero, hemos detectado las fuentes haciendo uso de *Source Extractor*, y las hemos clasificado. Hemos calculado la diferencia de color para diferentes filtros y realizado diagramas color-color. Este último proceso también ha sido hecho con un catálogo perteneciente a Arrabal et al., el cual fue usado como referencia debido a su gran cantidad de LAEs. Comparando ambos diagramas, hemos seleccionado una zona en el nuestro donde buscar posibles LAEs pertenecientes a un protocúmulo.

A pesar de nuestros esfuerzos, no hemos conseguido un resultado absoluto. La densidad de superficie no es muy buena, y todo indica una posible contaminación en los datos. Además, para poder asegurar que los candidatos son LAEs, un análisis de espectroscopía debería hacerse, no obstante, esto va más allá de nuestro proyecto.

Algo que si podemos confirmar es que el uso de filtros de media banda no son los más indicados para buscar este tipo de objetos.

5.2 Conclusions

We have analysed a region of the sky searching for protoclusters. First, the detected all the sources using Source Extractor, and then classified them. We have calculated the colour difference for different filters, a plotted colour-magnitude and colour-colour diagrams. This last process was also done with the catalogue lent by Arrabal et al., which was used as a reference for LAEs searching (as it contained this type of galaxies in our redshift range). Comparing the diagrams, we have selected a zone in ours which matches the one containing the LAEs in the reference diagrams and have selected our protocluster candidates from that region.

Despite our effort, an absolute result cannot have been achieved at this stage of the project. The obtained surface density for our catalogue was not good enough, and the plots indicate that a possible contamination of the data (both, Arrabal et al.'s and ours) have occurred. Finally, in order to assure that our candidates are LAEs, a further analysis using spectroscopy of the galaxies should be done, however it goes beyond this course's project.

Something that we can conclude is that the use of medium band filters is not the best way to look for this kind of objects. Bunker et al.'s models application with these filters (all of them of a very similar FWHM) was unsuccessful, and the model of Chanchaiwowarit etl al., despite also made using SHARDS filters to search for LAEs, the filters they used also had a significant difference in their FWHM.

6 Acknowledgements

6.1 Agradecimientos

Me gustaría dar las gracias a la familia y amigos por el apoyo aportado, y al propio tutor del proyecto, quien a veces creía más en mí que yo mismo. También nos gustaría agradecer a Arrabal et al. Su ayuda permitiéndonos el uso de su catálogo para nuestra investigación.

6.2 Acknowledgements

This project could have not been possible without the support of family and friends, and tutor itself, who believed in me more than myself. Also, we would like to thank Arrabal et al. for lending their catalogue to be used in order to progress in the project.

7 Annex – Secondary diagrams

7.1 Resumen

Como se indicó en secciones anteriores, presentamos aquí algunos diagramas que hicimos para clasificar los objetos no obstante no se usaron al final para la obtención de resultados.

7.2 Secondary diagrams

As stated in previous sections, we present now some diagrams that we used using other classification criteria however they were not to obtain our ultimate results. Diagrams here are of the kind colour-magnitude (as used by Bunker et al.) or diagrams showing only LAEs and LBGs from Arrabal et al.'s catalogue.

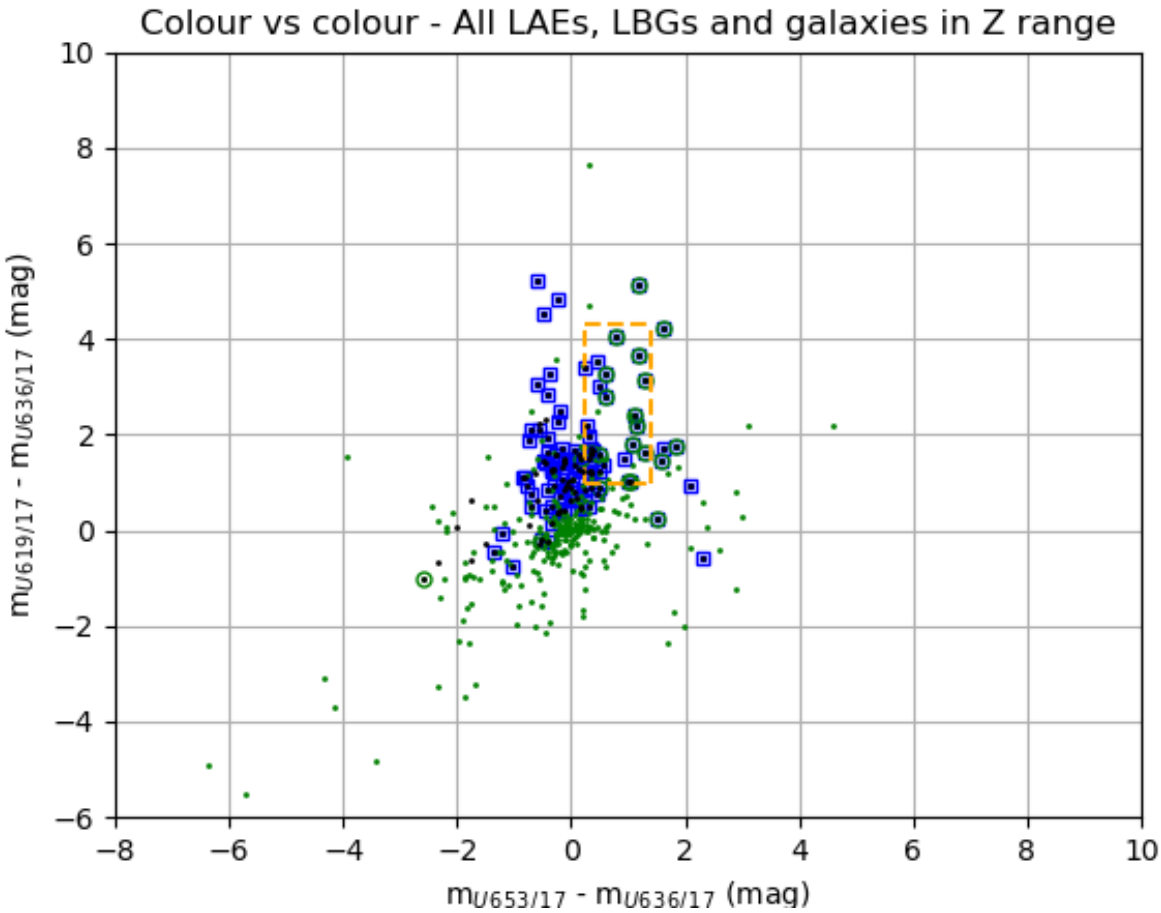

Figure. 13. LAEs, LBGs and objects in redshift range from Arrabal et al.'s catalogue. Black dots indicate galaxies in redshift range while green dots LAEs outside the redshift range. Green circles and blue squares use the same legend as in previous Fig.s.

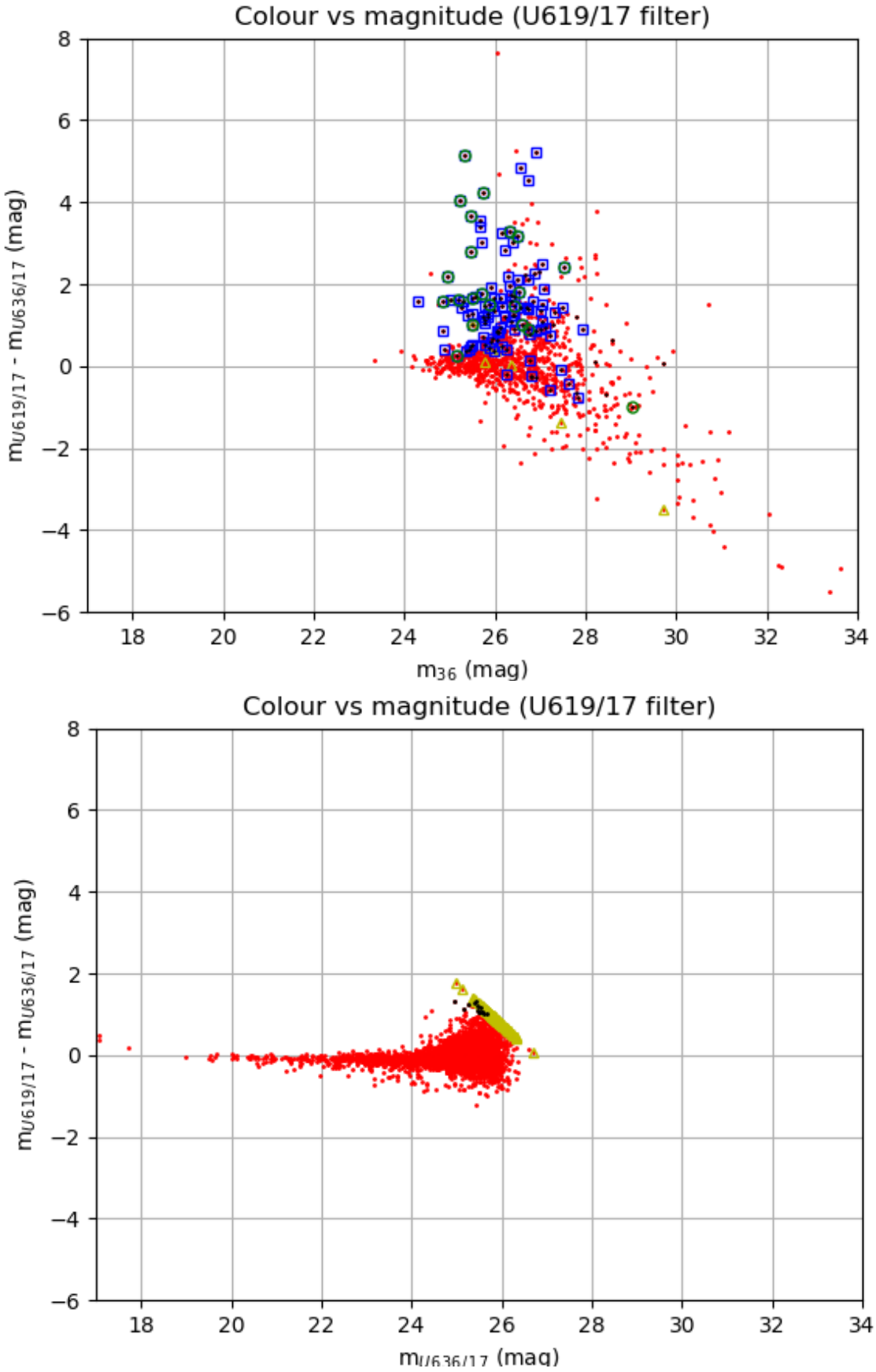

Figure. 14. Colour-magnitude fiagrams for the U619/17. Top pannel shows Arrabal et al.'s. botton pannel shows ours. Same legend as in previous Fig.s (exception: botton pannel shows som balck dot which indicates the well-deetected obejcts in the selection region). It must be noted the displacement previously mentioned. It must be noted the magnitude displacement, going in the x-axis from 24 to 34 mag in the top pannel while the bottom pannel it goes from 17 to 26.

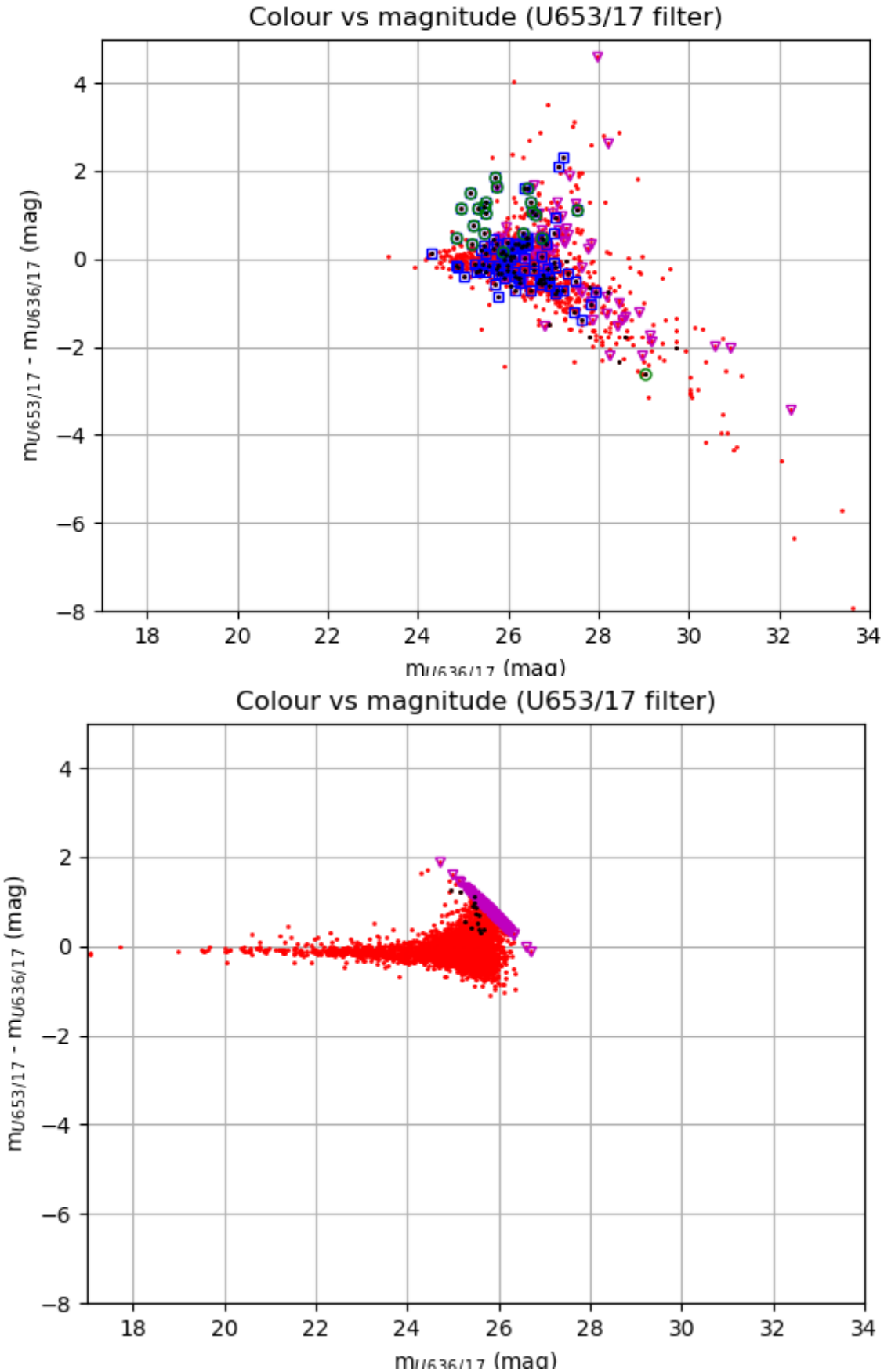

Figure 15. Colour-magnitude fiagrams for the U653/17. Top pannel shows Arrabal et al.'s. botton pannel shows ours. Same legend as in Fig. 14. Again, it must be noted the displacement previously mentioned. Also, the magnitude displacemente must be noted again (nearly same limits than in Fig. 14)

8 References

[1] Arrabal et al., 2018, "*A SIMULTANEOUS SEARCH FOR HIGH-Z LAES AND LBGS IN THE SHARDS SURVEY*", MNRAS, 000, 1

[2] Bunker et al., 1995, "*ON NEAR INFRARED Ha SEARCHES FOR HIGH-REDSHIFT GALAXIES*", MNRAS, 273, 513

[3] Chanchaiwowarit et al., 2017, "*GRAN TELESCOPIO CANARIAS OBSERVATIONS OF AN OVERDENSE REGION OF LYMAN A EMITTERS AT Z = 6.5*", MNRAS, 469, 2646

[4] Cox et al. 2011, "*GAS AND DUST IN A SUBMILLIMETER GALAXY AT z = 4.24 FROM THE HERSCHEL ATLAS*", ApJ, 740, 63

[5] Daddi; Dannerbauer et al., 2009, "*TWO BRIGHT SUBMILLIMETER GALAXIES IN A Z = 4.05 PROTOCLUSTER IN GOODS-NORTH, AND ACCURATE RADIO-INFRARED PHOTOMETRIC REDSHIFTS*", ApJ, 694, 1517

[6] Eales et al., 2010, "*THE HERSCHEL ATLAS*", PASP, 122, 499

[7] Holwerda, 2005, "*SOURCE EXTRACTOR FOR DUMMIES*", Astromatic.net

[8] Overzier, 2016, "*THE REALM OF THE GALAXY PROTOCLUSTERS. A REVIEW*", AAR, 24, 1

[9] Pérez-González et al., 2012, "*SHARDS: AN OPTICAL SPECTRO-PHOTOMETRIC SURVEY OF DISTANT GALAXIES*", ApJ, 762, 46

[10] Rodriguez Espinosa, 2014, "*EPISODIC STAR FORMATION IN A GROUP OF LAES AT Z = 5.07*", MNRASL, 444, L68

[11] Smail; Ivison; Blain, 1997, "*A DEEP SUB-MILLIMETER SURVEY OF LENSING CLUSTERS: A NEW WINDOW ON GALAXY FORMATION AND EVOLUTION*", ApJ, 490, L5

[12] Walter et al., 2012, "*THE INTENSE STARBURST HDF850.1 IN A GALAXY OVERDENSITY AT Z = 5.2 IN THE HUBBLE DEEP FIELD*", Nature, 486, 233